



Bulletin of the Mineral Research and Exploration

<http://bulletin.mta.gov.tr>



Porphyry copper prospectivity mapping using fuzzy and fractal modeling in Sonajeel area, NW Iran

Zahra YAZDI^a, Alireza JAFARI RAD^{a*}, Mehraj AGHAZADEH^b and Peyman AFZAL^c

^a Department of Geology, Science and Research Branch, Islamic Azad University (IAU), Tehran, Iran

^b Department of Geology, Payame Noor University, Tabriz, Iran

^c Department of Mining Engineering, South Tehran Branch, Islamic Azad University (IAU), Tehran, Iran

Research Article

Keywords:

Fuzzy logic, fractal, GIS, prospectivity map, porphyry copper, sonajeel.

ABSTRACT

Main purpose of this research is to present a local scale GIS-based mineral prospectivity model for prospecting Cu porphyry mineralization, and to validate the produced model by field observation, surface sampling and drilling data. Sonajeel area which is the subject of this study is a part of Arasbaran mineralization belt, NW of Iran. Constructing a mathematical exploratory algorithm based on a mineralization type is a complicated and interdisciplinary task. For this purpose, results from processing and interpreting different data sets including geology, geochemistry and remote sensing were considered. A comprehensive exploratory integration model was built up considering the exploration stage and the descriptive porphyry mineralization model suggested by Sillitoe (2010). In order to prepare inputs for GIS-based exploration model, value assigned grids or evidence layers were produced using fuzzy membership curves and then integrated via gamma fuzzy function. In addition, for defuzzification and prioritizing the mineral prospectivity map, a Concentration-Area (C-A) fractal model was applied on the pixel values of the prospectivity map. Finally, the results were confirmed via field observation, surface sampling and drilling. Borehole logs at the first priority displayed a Cu mineralization zone with an average grade of 0.5%.

Received Date: 29.08.2017

Accepted Date: 04.01.2018

1. Introduction

Mineral prospectivity mapping (MPM) is carried out based on integration of evidence layers especially at reconnaissance and prospecting scales in mineral exploration (Carranza, 2009 *a,b*; Jafarirad, 2009; Porwal and Carranza, 2015; Yousefi and Carranza, 2014, 2015a,b). Each scale is characterized based on the accuracy of evidence maps, where level of accuracy increases with the acceleration of exploration scale. An MPM is drawn in a Geospatial Information System (GIS) environment by different methods (Agterberg et al., 1990; Almasi et al., 2015a,b; Bonham-Carter et al., 1989; Bonham-Carter, 1994; Carranza et al., 2008; Carranza, 2014; Chung and Agterberg, 1980; Chung and Moon, 1990; Jafarirad and Busch, 2011; Lusty et al., 2012; Magalhaes and Souza Filho, 2012; Nykanen et al., 2008; Parsa et al., 2016; Parsa et al.,

2017; Yousefi, 2017). In every scale, data layers are collected, processed and integrated using a variety of available functions (Abedi et al., 2017; Almasi et al., 2015a,b; Yazdi et al., 2014). In this research, evidence layers including geology, geochemistry, structure and alteration have been produced individually and then checked using field observation. Subsequently, evidence maps were integrated in order to find high potential locations of porphyry copper mineralization in the Sonajeel system, NW Iran. Finally, the MPM has been evaluated and validated by field observation and drilling data.

A wide variety of volcanic, sedimentary and metamorphic units host porphyry copper deposits worldwide, which displays the almost ineffectiveness of the host rock in their mineralization (Sillitoe, 2010). Cross-cutting faults play a major role in the size,

* Corresponding author: Alireza JAFARI RAD, alirad@yahoo.com
<https://dx.doi.org/10.19111/bulletinofmre.391835>.

geometry and setting of the deposits. All the porphyry copper deposit models that has been suggested so far place the potassic alteration at the core of the porphyry system. Moreover, geochemical halo of Zn usually engulfs porphyry mineralization systems.

Iran inherited its mineral endowment from the processes involved in its lithospheric evolution and plate tectonics (Berberian and Kings, 1981; Stocklin 1974). Subduction zones which host porphyry copper mineralization (PCM) constitutes a major part of Iran (Afzal et al., 2012; Aghazadeh et al., 2015; Hassanpour and Afzal, 2013; Jamali and Mehrabi, 2015; Richards and Sholeh, 2016). Post collisional Neo-Tethys oceanic closure process caused the vast and huge magmatism along South to North West of Iran (Aghazadeh et al., 2015; Babaie et al., 2001; Karimzadeh Somarin, 2005; Pazand et al., 2012). This Oligo-Miocene magmatic domain has been suggested to be divided in to two main belts (Moritz et al., 2015). NW-SE trending Urumieh-Dokhtar magmatic arc hosts some well-known deposits namely Sarcheshmeh, Meiduk and Kahang (Afzal et al., 2010; Aghazadeh et al., 2015; Jafarirad, 2009; McInnes et al., 2003; Shahabpour and Keramers, 1987; Yazdi et al., 2014). Arasbaran belt, with a WNW-ESE trending

located in NW of Iran, hosts Iran’s giant Cu porphyry mine Sungun, and is considered as a top priority potential for finding new deposits (Aghazadeh et al., 2015; Jamali and Mehrabi, 2015). Sonajeel system, the area subjected to this study, is located in the east of the Arasbaran belt (Figure 1).

Several exploration and geological surveys have been done on the Sonajeel mineralization (Hezarkhani, 2008; Hosseinzadeh et al., 2009; 2017; Karimi et al., 2009; Pazand et al., 2013).

Sonajeel system comprises Oligo-Miocene quartz monzodiorite and granodiorite intrusives, and is similar to Sungun and other PCM prospects of Arasbaran belt. Rock exposures in this prospect consist of Eocene volcano-sedimentary units, Oligo-Miocene intrusives and Quaternary volcanic rocks (Figure 1). Eocene volcano-sedimentary units which were deposited in the marine and continental areas, include andesitic to basaltic lava, basaltic to andesitic volcanic rocks, ignimbrite and tuff. Eocene volcano-sedimentary units were intruded by various Oligo-Miocene intrusions including Sonajeel porphyry stock. This stock caused the percolation of hydrothermal fluids and has been suggested as the main factor in

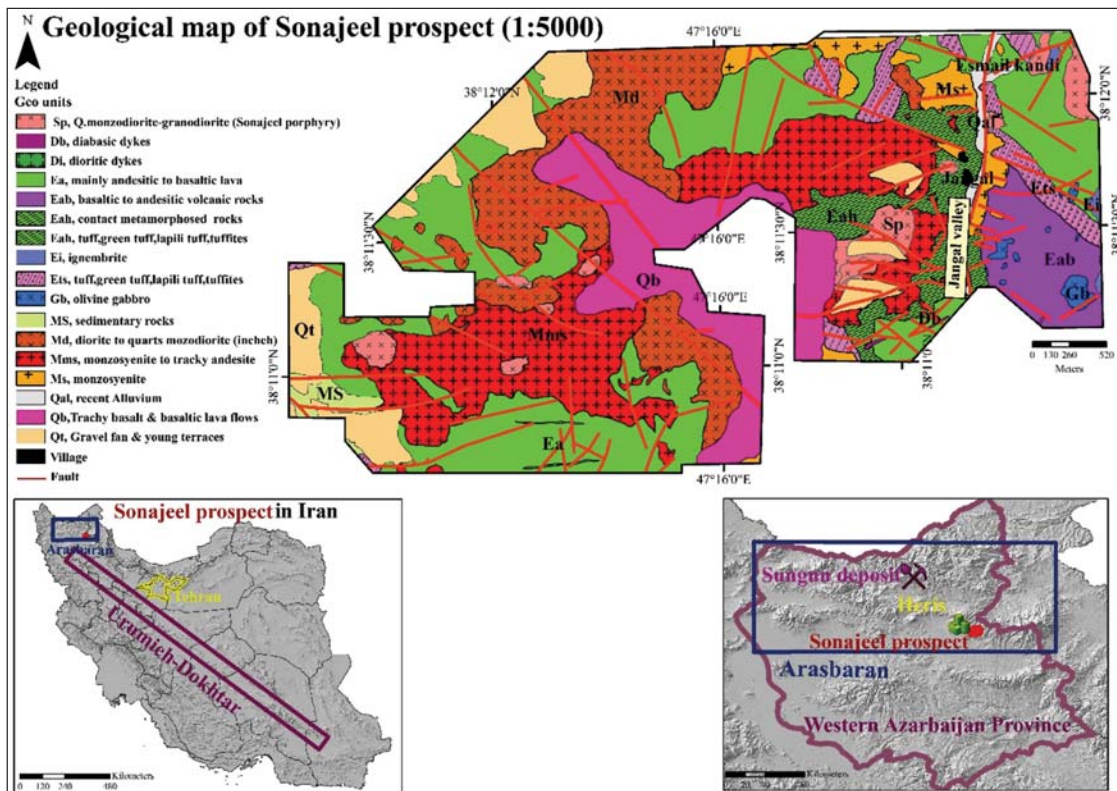


Figure 1- Geological map (1:5000) of the Sonajeel system (after Aghazadeh, 2014)

Sonajeel mineralization (Aghazadeh et al., 2015). Intrusive units are distributed in the forms of stock, sill, dyke and vein in the study area. Quaternary units including tracky basalt and basaltic lava flows, gravel fans and recent alluvium and Eocene volcanic rocks with different thicknesses, cover the older units.

Fault systems in this area have been divided into two main groups as follows (Aghazadeh, 2014):

1- Old deep first order NW-SE system that is related to the Tabriz and Goshadagh faults and has been suggested as the controlling factor of the emplacement of intrusive units.

2- NE-SW system that influenced dykes and quaternary volcanism.

Therefore, fault systems have influenced intrusions and alterations which are major factors for this mineralization.

2. Materials and Methods

Porphyritic igneous bodies are mostly I-type metalliferous intrusions. These bodies are typically calc-alkaline with medium potassium content or rarely alkaline with high potassium content. Their composition range from calc-alkaline diorite and quartz-diorite, to alkaline granodiorite, quartz-

monzonite and diorite, to monzonite and syenite (Seedorf et al., 2005). In Sonajeel area, from the alteration and geochemistry perspective, mineralization signatures totally obey global porphyry genetic models.

Geological and structural map of the study area were produced at 1:5000 scale by Coome Madan Company in 2014. Furthermore, alteration zones were detected using remote sensing techniques from ASTER and QuickBird images. Geochemical data used in this paper were obtained by lithochemical samples which were collected by Kavoshgaran Company in 2006 (Table 1).

In this study, SPSS 24, Microsoft office excel 7, ENVI 5.1 and ArcGIS 10.2.1 software were employed for statistical analyzes, image processing, producing and integrating evidence maps respectively. In this paper, firstly data layers were processed separately, then controlled via field confirmations. Moreover, evidence maps were generated using fuzzy membership functions, then were integrated via fuzzy logic method. Finally, the integrated map was classified by Concentration-Area (C-A) fractal model and results evaluated by field checking. The first two priorities were suggested for further exploration at 1:1000 scale and drilling. These steps are introduced briefly in the form of a flow chart in figure 2.

Table 1- Lithochemical samples.

Laboratory name	Total samples	Method	Date	Number of elements	Elements
AMDEL (Australia)	1248	For all samples except Gold: ICP Mass Gold: F.A.	2006	44	Ag, Al, As, Au, Ba, Be, Bi, Ca, Cd, Ce, Co, Cr, Cs, Cu, Fe, Hg, K, La, Li, Mg, Mn, Mo, Na, Nb, Ni, P, Pb, Rb, Re, S, Sb, Sc, Sn, Sr, Te, Th, Ti, Tl, U, V, W, Y, Zn, Zr

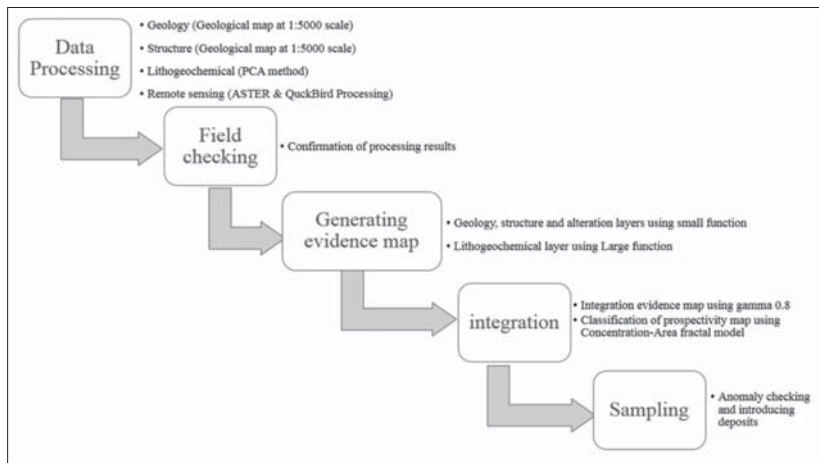


Figure 2- Processing Flowchart.

Used fuzzy membership functions, and the fuzzy operator which was employed for integration, are explained in a summarized format below.

2.1. Small Fuzzy Membership Function

The small fuzzification function has been defined as following equation:

$$\mu_x = \frac{1}{1 + (\frac{x}{f_2})^{f_1}} \tag{1}$$

Where f_1 is the spread of the transition from a membership value of 1 to 0 and f_2 is the midpoint (Tsoukalas and Uhrig, 1997).

2.2. Logistic Fuzzy Membership Function

Logistic function could be generator of fuzzy membership for spatially continuous weights (Bishop, 2006; Nykänen et al., 2008; Yousefi et al., 2012; 2013; 2014; Yousefi and Carranza, 2015a, b; Yousefi and Nykänen, 2016). This function has been detected as following equation (Yousefi and Carranza, 2015a):

$$\mu_x = \frac{1}{1 + e^{-s(x-i)}} \tag{2}$$

Where i and s are inflexion point and slope of the logistic function, which determined as following equations (Yousefi and Nykänen, 2016):

$$s = \frac{9.2}{X_{MAX} - X_{MIN}} \tag{3}$$

$$i = \frac{X_{MAX} + X_{MIN}}{2} \tag{4}$$

Where X_{min} and X_{max} are the minimum and maximum evidential values respectively.

2.3. Gamma Fuzzy Operator

The gamma operator is the general form of fuzzy Sum (An increaser function, used when the combination of multiple evidences is more important or larger than any of the inputs alone) and fuzzy Product (A reducer function, used when the combination of multiple evidence is less important or smaller than any of the inputs alone). This operator has been shown in equation 5 (Tsoukalas and Uhrig, 1997):

$$\mu_{Combination} = \left(\prod_{i=1}^n \mu_i \right)^\delta \left(1 - \left(\prod_{i=1}^n (1 - \mu_i) \right) \right)^{1-\delta} \tag{5}$$

Where $\mu_{Combination}$ = each unit value in output map

μ_i = the weight of i th factor map

2.4. Concentration-Area (C-A) Fractal Model

Cheng et al. (1994) proposed an element concentration–area (C–A) model, which may be used to define the geochemical background and anomalies. The model has the general form:

$$A(\rho \leq v) \propto \rho^{-a1} ; A(\rho \geq v) \propto \rho^{-a2} \tag{6}$$

Where $A(\rho)$ denotes the area with concentration values greater than the contour value ρ ; v represents the threshold; and $a1$ and $a2$ are characteristic exponents. Using fractal theory, Cheng et al. (1994) derived similar power-law relationships and equations in extended form (Afzal et al., 2010; 2012; Almasi et al., 2015a,b).

2.5. Principal Component Analysis (PCA)

Principal component analysis (PCA) is a multivariate technique that reduced variables by several inter-correlated quantitative dependent variables (Abdi & Williams, 2010). Among the advantages of PCA can cite that it's possible to determine the correlation of each PC with each of the original variables, it enables us to find outliers and groups of variables and allows us to reduce the dimensionality of the problem by the elimination of some variables in the next steps of the mineral exploration, if we consider that they are not helping to explain the processes interpreted via PCs.

3. Evidence Maps

3.1. Geological Layer

Sonajeel porphyry intrusive units composed of quartz-monzodiortic to granodioritic rocks, which were suggested as the key mineralization factor are similarly comparable to other porphyry copper deposits and prospects in Arasbaran belt (Aghazadeh et al., 2015). These intrusive units are in the form of stock and apophyse have outcrops around Jangal and Esmailkandi villages in the east of the study area (Figure 1). Sonajeel porphyry intrusive units has been intruded into the Eocene rocks and micromonzosyenite rocks (Figure 3a) which indicated Oligo-Miocene age. These intrusive rocks contain potassic and phyllic alteration in the surroundings of Jangal village and

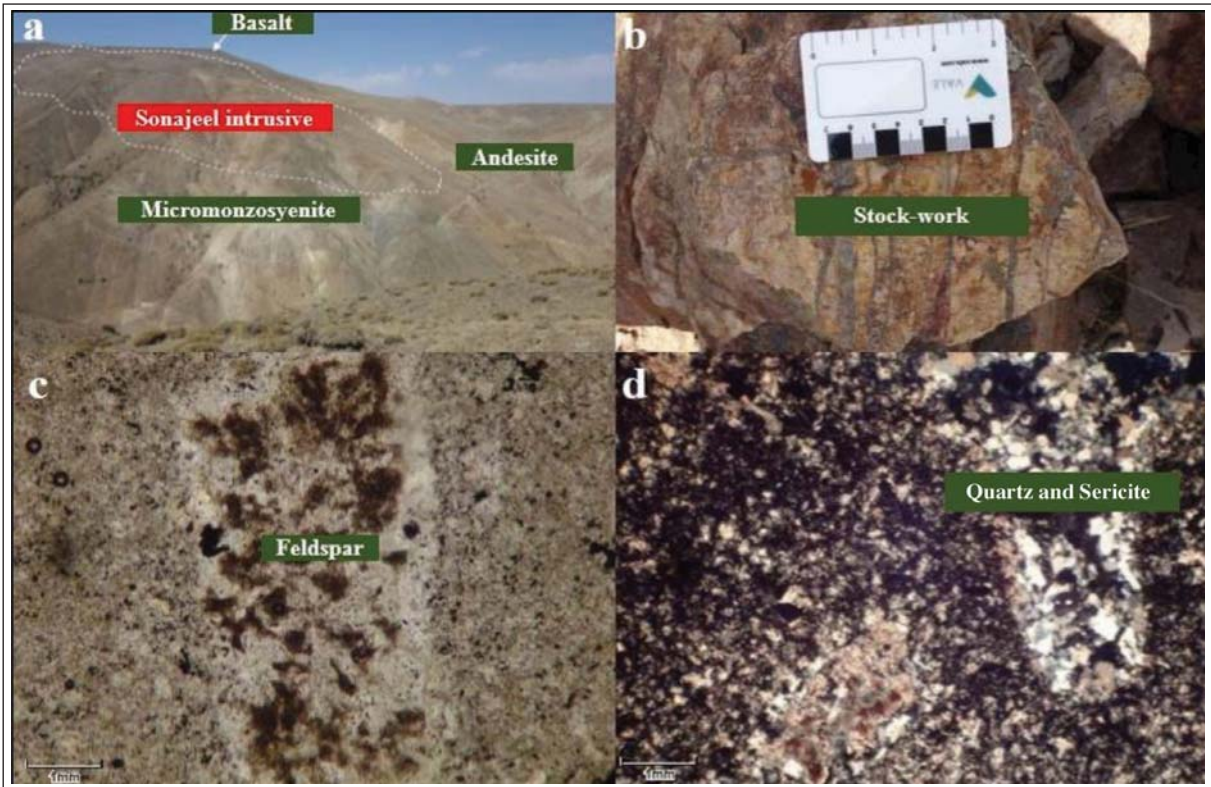


Figure 3- (a) Sonajeel porphyry intrusive (b) distribution of Stock-work in the Sonajeel porphyry intrusive (c) porphyritic texture with feldspar phenocryst in the sample of Sonajeel porphyry intrusive, PPL (d) spreading Quartz and Sericite due to affecting of phyllic alteration, XPL.

have stockwork mineralization indications (Figure 3b). The texture of this intrusive is porphyritic with feldspar and phenocrysts of mafic minerals.

Ten thin sections have been studied from these lithologies (Figure 3 c and d). The sample presented here has porphyritic texture with feldspar phenocrysts which has been affected by sericitic alteration. These phenocrysts are distributed in quartz, sericite and secondary biotite background. Sericitic alteration has covered the primary potassic alteration meanwhile some of its biotite has remained intact.

In order to produce the source rock evidence layer, firstly, Euclidian distance map of Sonajeel porphyry intrusives was built due to importance of proximity to these intrusive units in the porphyry models. Afterwards, fuzzy membership of this distance map has been generated using small function with midpoint 400 and spread 5 (Figure 4). This evidence map has been classified using C-A fractal model which is presented in figure 5.

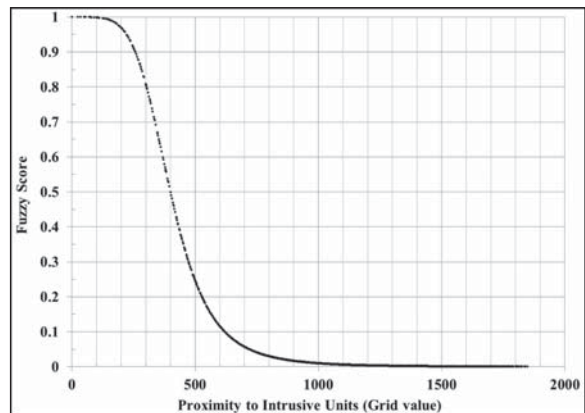


Figure 4- Fuzzy membership of intrusive .

3.2. Structural Layer

Structures play a significant role in porphyry mineralization (Byron and Berger 2008; Richards, 2015). In the study area, structural mapping have been done at 1:5000 scale which mostly of indicated faults is strike-slip and have NW-SE trends (Figure 6). Fuzzification algorithm used in this layer is small with midpoint and spread 200 and 7 respectively (Figure 7).

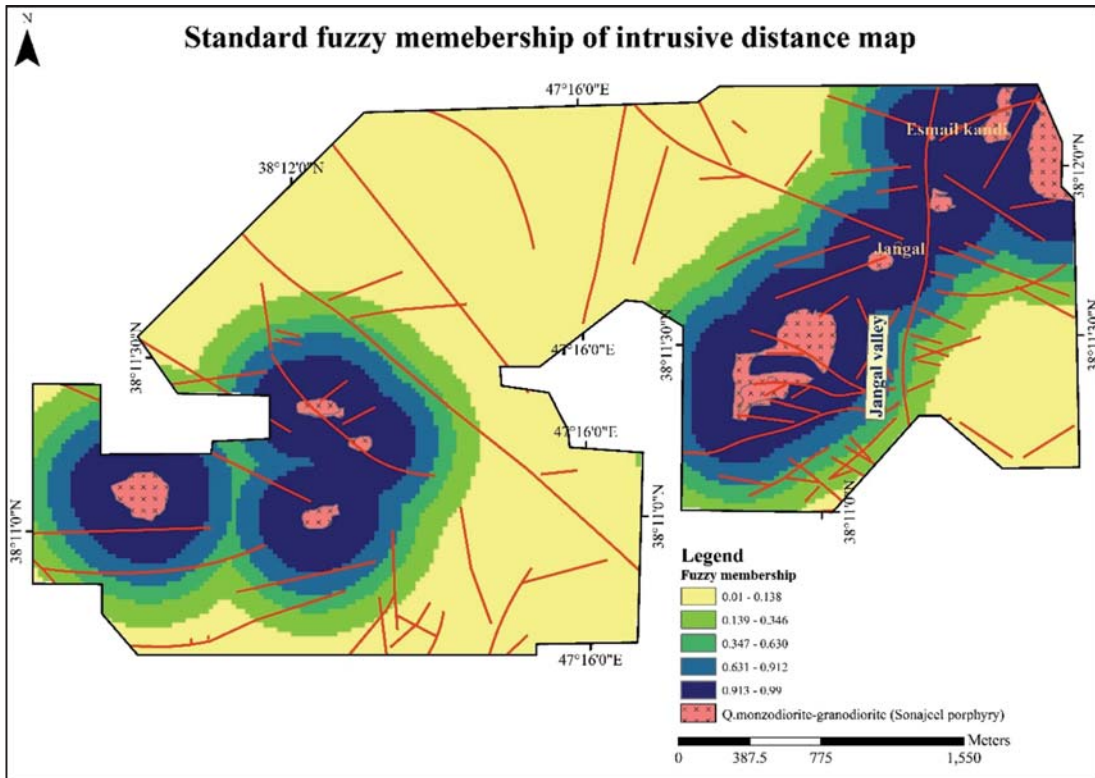


Figure 5- Evidence map of intrusive rocks as the mineralization producer.



Figure 6- One of the strike-slip fault in the study area which shifted dyke.

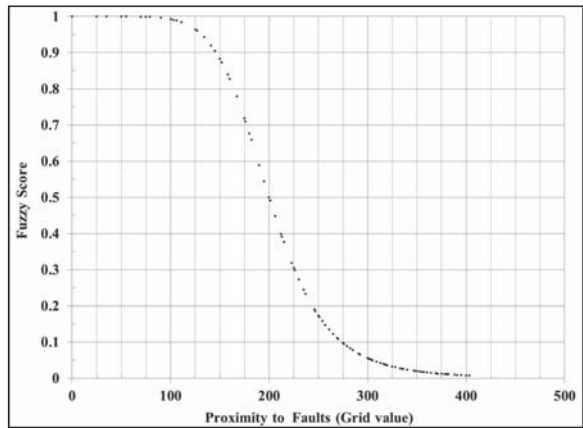


Figure 7- Fuzzy membership of faults.

Moreover, thresholds for classification of this evidence map have been calculated using Concentration-Area fractal method (Figure 8).

Fault concentrations are vastly dispersed in Sonajeel porphyry intrusive units (east of Jangal valley) which is a basic factor in rising hydrothermal fluids and mineralization. This fact has been confirmed by field evidences in the Sonajeel porphyry system.

3.3. Alteration Layer

Hydrothermal fluids broadly effect rocks and produce specific alteration zones including potassic, phyllic, argillic and propylitic in porphyry copper systems (Alimohammadi et al., 2015; Beane, 1982; Berger et al., 2008; Byron and Berger, 2008; Lowell and Guilbert, 1970; Meyer and Hemley, 1967; Silitoe, 2010; Sillitoe, 2010). Mineralization is related to potassic and phyllic alteration in the Sonajeel

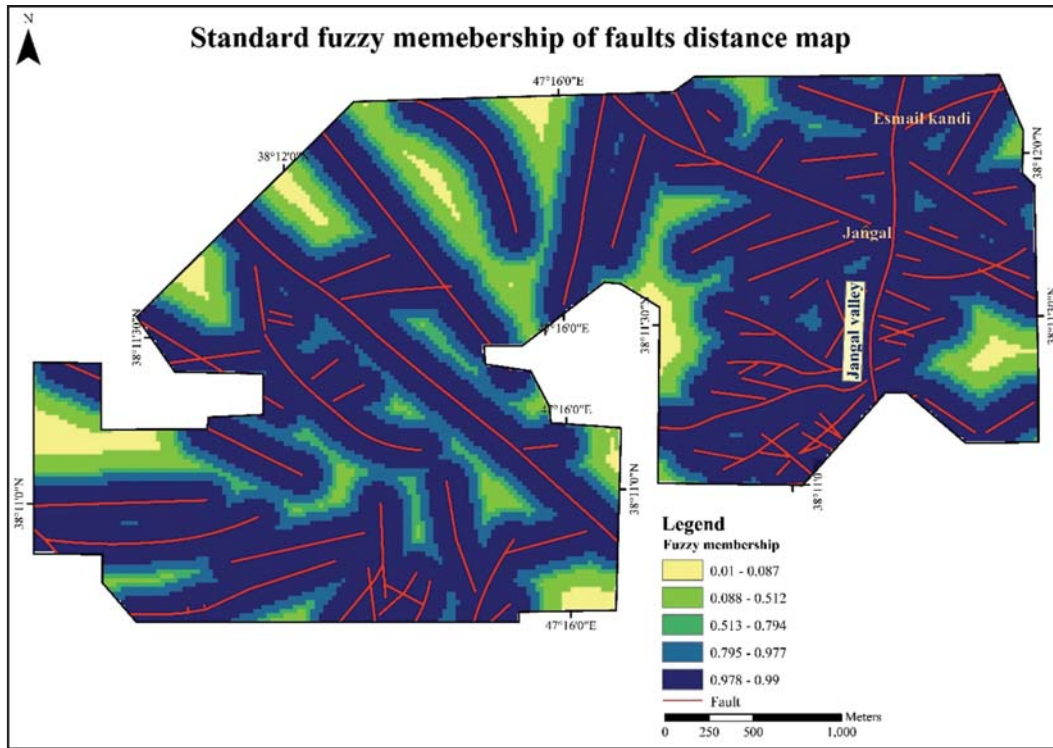


Figure 8- Evidence map of faults.

system which was outlined using remote sensing. For this purpose, Thermal Emission and Reflection Radiometer (ASTER) multispectral image has been geometrically corrected using QuickBird image with pixel width of about 0.5 m as a reference image in order

to improve the rectification process. Alteration zones have then been detected using Relative Absorption Band-Depth grids (RBD) method. Afterwards, the image processing results have been evaluated by field evidences (Figure 9). Finally, distance map of potassic

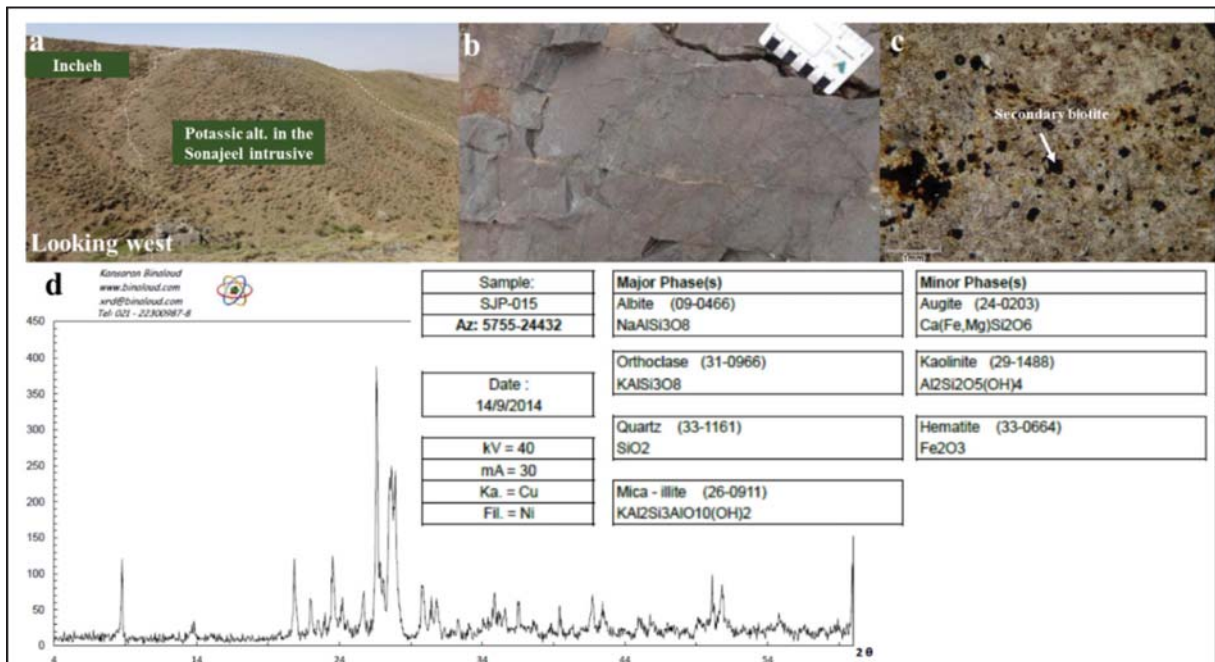


Figure 9- a) potassic alteration in Sonajeel porphyry intrusives (b) gray sample of potassic alteration (c) Thin section of potassic alteration which contains secondary biotite and feldspar in the microgranular background (d) XRD report of one of the potassic sample.

and phyllic alterations have been produced and fuzzy memberships have been individually created using small fuzzy function with midpoint of 300 and spread of 5 (Figure 10, 11 and 12). Potassic and phyllic alterations were directly observed and are distributed in the east of Jangal valley similar to the faults and intrusive units.

3.4. Lithochemical Layer

Multivariate principal component analysis method is used for determining elemental correlations and elemental paragenesis (Afzal et al., 2010; Davis, 2002; Deng et al., 2007, 2008). PCA method has reduced dimensions and is commonly used in the geochemical studies (Carranza and Hale, 2002; Carranza, 2010; Wang et al., 2011, 2012, 2013, 2014). In this paper, lithochemical samples (with 100 m*100m cells) have been processed using PCA method and resulted in 2 factors including Cu- Zn and Mo- As- Pb. Afterwards, fuzzification was on Cu- Zn performed using Logistic method in order to produce geochemical evidence layer. Inverse Distance Weighted (IDW) technique was used for interpolation and gridding. As mentioned in the methodology part, copper and zinc have a high correlation coefficient. An observable evidence of that is their overlapping anomalies in the east of Jangal valley (Figure 13).

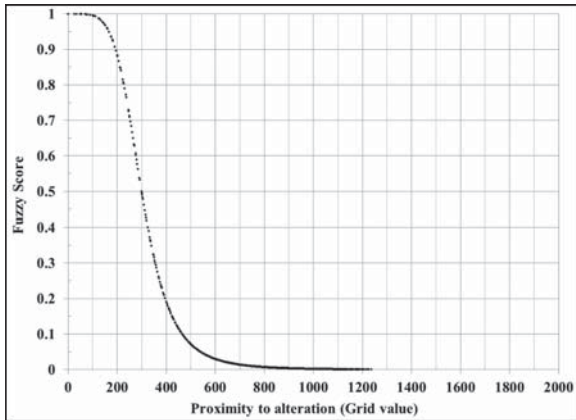


Figure 10- Fuzzy membership of alteration.

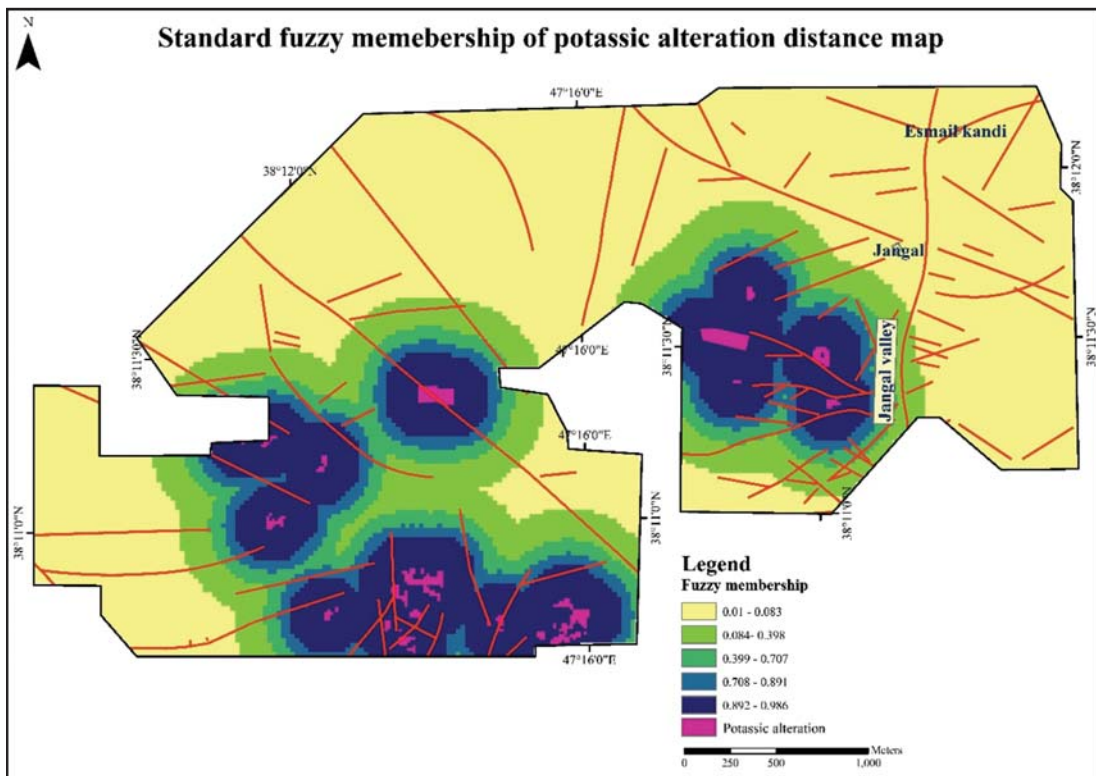


Figure 11- Evidence map of potassic alteration.

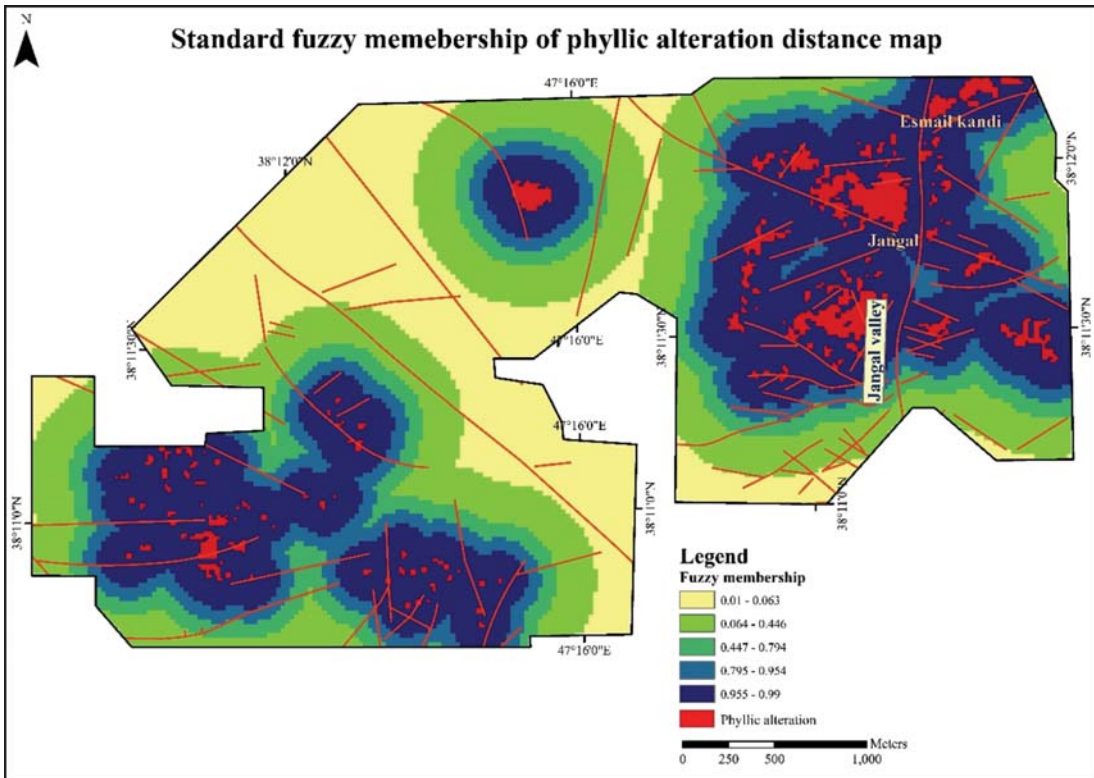


Figure 12- Evidence map of phyllic alteration.

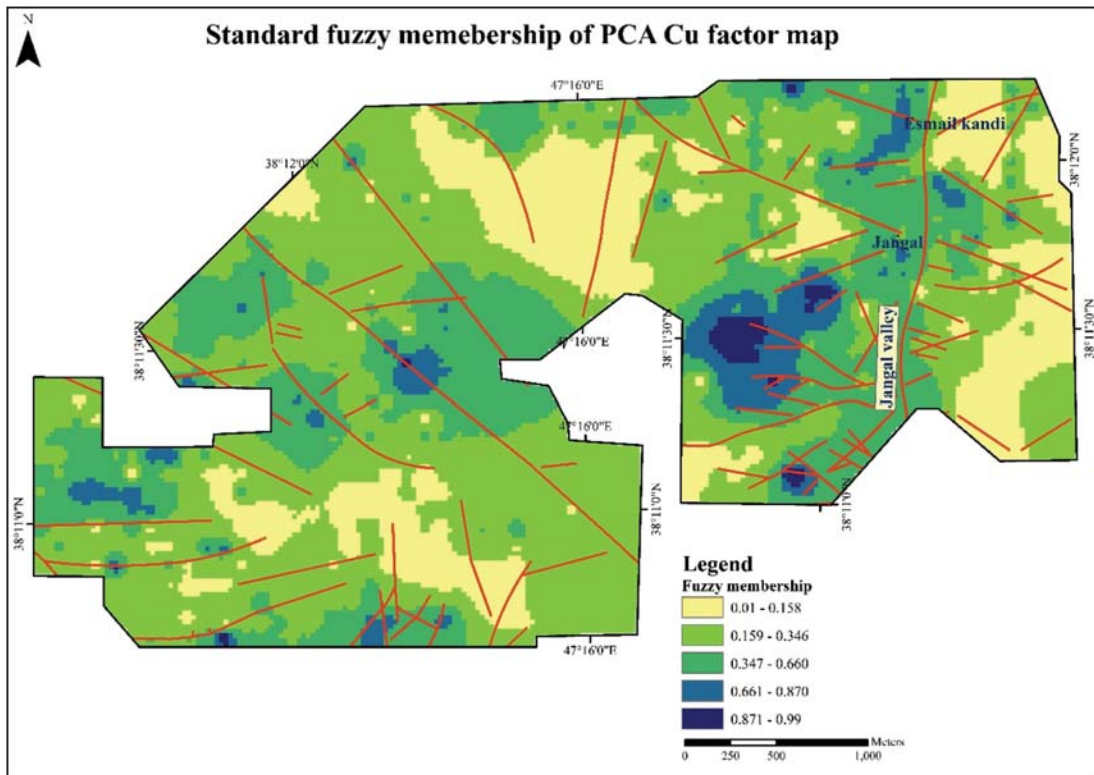


Figure 13- Evidence map of geochemistry.

4. Integration

In knowledge-driven methods, experts (with different fields and levels of expertise) integrate different pieces of information for mineral prospectivity mapping. Assigning integers to different geological features or to several intervals of a grid (e.g. geophysical or geochemical), is a procedure that has been practiced in a voluminous studies of this kind. In this method, a major issue is the controversies which arouse over assigning discrete values to the intervals. To overcome this issue, more recent studies focused on applying functions and curves for preparing integration input grids or evidence layers. These functions commonly situate in the paradigm of the fuzzy theory and convert a set of data into a grid ranging from ~0.01 to ~0.99. Fuzzy operators such as fuzzy and, fuzzy or and fuzzy gamma are among the techniques used for integrating evidence maps.

The fuzzy logic method as one of the knowledge-driven methods is widely accepted for producing MPM. It was firstly used by An et al. (1991) and is still employed in mineral exploration (Ford et al., 2015; Joly et al., 2012; Porwal and Kreuzer, 2010; Lisitsin et al., 2013; Lusty et al., 2012; Nykänen et al., 2008; Parsa et al., 2016; Parsa et al, 2017). In this paper gamma (0.8) operator has been used for combining evidence maps. It is a combination of both sum and

product algorithms. Subsequently, the created fuzzy logic MPM has been prioritized using Concentration-Area (C-A) fractal model (Figure 14: Almasi et al., 2015a,b, 2017).

5. Results and Discussion

Data analysis proves that Sonajeel porphyry system has the adequate potential for becoming a PCM. Its surface indications are: potassic alteration zone, wide stock-work system, and Sonajeel porphyry intrusive units. The produced MPM has been validated via field observations and sampling (Figure 15). Samples were mainly studied using two techniques 1) ICPMS and 2) polished sections. The average Cu grade received from ICPMS analysis was 0.4 percent, a satisfactory grade for surface samples in this scale of exploration. Maximum grade was 2 and Minimum grade of the samples was 0.1 percent.

Several polished section samples have been studied from the identified priorities. SJP011PS sample which represent the supergene zone contains chalcocite (Cu₂S) and covellite (CuS). These minerals display the replacement of the primary sulfide minerals such as bornite (Figure 16). SJP06PS sample contains bornite and chalcopyrite primary and secondary sulfide minerals which had been altering to chalcocite and covellite iron hydroxide. Iron oxide (magnetite) has

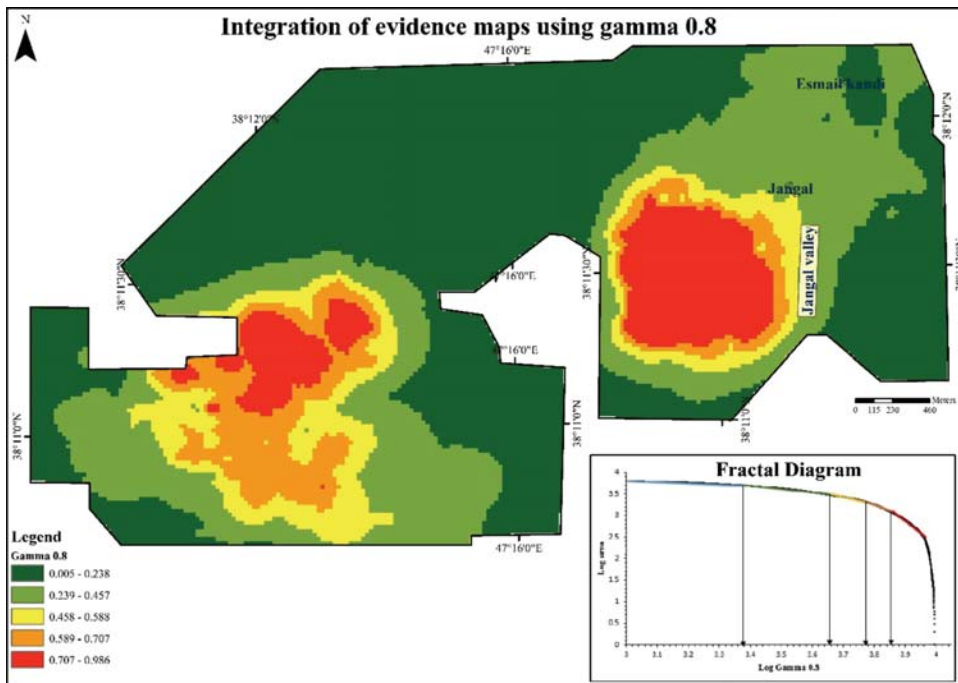


Figure 14- Ranking MPM using C-A fractal method.

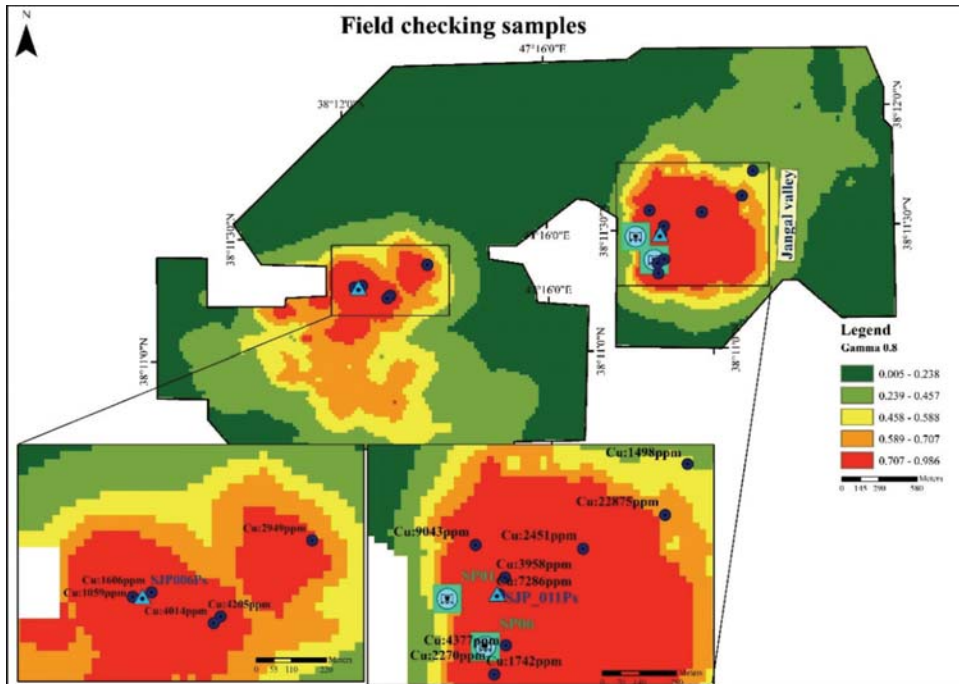


Figure 15- Location of sampling in the field checking.

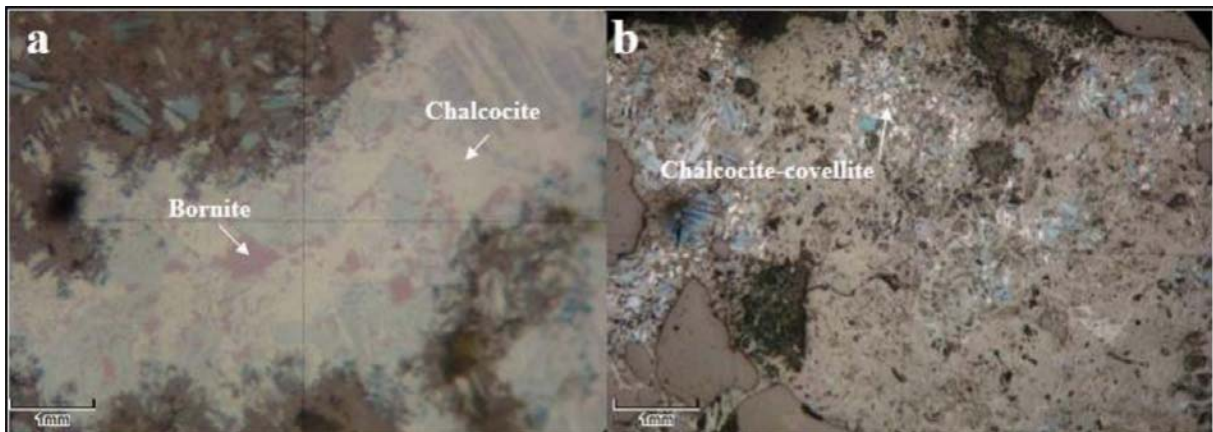


Figure 16- SJP011PS sample (a) replacement of bornite by chalcocite, PPL (b) spread of chalcocite and covellite.

primary occurrence in the background of this sample. This sample displays the boundary of the hypogene and supergene zones (Figure 17).

After positive results from the samples' analysis, two boreholes were drilled in the first identified priority, east of the study area (Jangal valley). Core sample analysis of the boreholes SP01 and SP06 contain average Cu concentrations of 2267 and 2959 ppm respectively. Lithological, alteration and Cu concentration logs are presented in figure 18. Borehole SP01 with the depth of the 400 meters, contain lithological units from quartzdiorite, granodiorite to andesite and andesite-basalt with mainly potassic

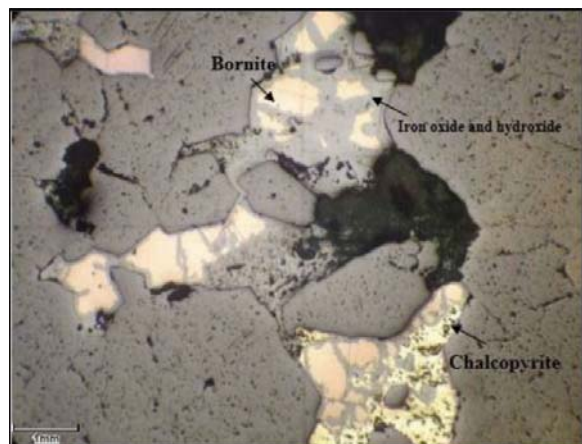


Figure 17- SJP06PS replacement of chalcopyrite and bornite by iron oxide and hydroxide.

and phyllic alterations. A direct relation between Cu concentrations and alterations are displayed. Borehole SP06 with the depth of 200 meters, shows alternation of potassic and phyllic quartzmonzonite. High grades of Cu are recorded at phyllic and especially potassic alteration zones (Figure 18).

6. Conclusion

In this research, the results from the analysis of the datasets (remote sensing and geochemical sampling) and the outcomes of the MPM were validated via field observation. Outlined prospects overlap with all the other anomalies in Jangal valley where the porphyry intrusive unit is exposed to the surface. Statistical analysis of the geochemical dataset displays a high elemental correlation between Cu and Zn which is compatible with global and regional porphyry deposit models.

Two exploratory boreholes which were drilled in the prospects (with the depth of 200 and 400 meters) explicitly displayed 200 to 300 meter porphyry mineralization with average copper concentration of 0.5 percent. A thorough drilling project with the purpose of reserve estimation is now active in the area.

Sonajeel porphyry intrusive units, which are suggested to be the main mineralization factor in the area, are comprised of quartz monzodiorite to granodiorite from Oligo-Miocene age. The outcomes of this paper displayed that, integration of the evidence layers is a valuable technique for determining and prioritizing surface priorities at every scale of mineral exploration. Moreover, validating the outcomes via field observations, sampling and sample analyzing is a necessity. It is a useful method for determining parameters the fuzzy function’s midpoint and spread. Remote sensing results showed that one of the most important data layers in porphyry copper exploration is delineated alterations. They can be determined using ASTER multispectral image. In addition, correcting the ASTER image via QuickBird image helped raising the geometrical accuracy. In processing geochemical data exploration, PCA method is suitable for decreasing the elemental variety and is very effective for finding elemental correlations.

Also, Concentration-Area (C-A) fractal method is suggested to be very effective for classification of the created MPM in different types of mineralization in any scale

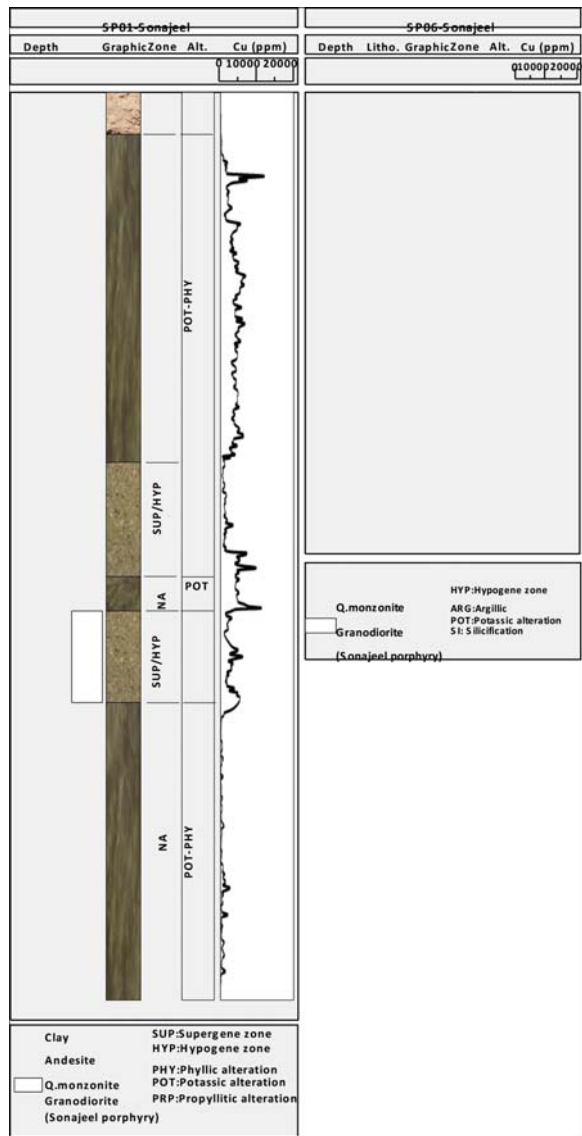


Figure 18- (a) SP01 log (b) SP06 log.

The two boreholes (with about 300 m depth) which was drilled on the first priority displayed 25 m copper mineralization with more than 0.5 percent Cu (BH013 & BH014).

Acknowledgements

We would like to acknowledge thorough reviews of Mr. Almasi and his comments. Also, we would like to express our gratitude to the Coome Madan Pars Company and the Speer Company for their supports.

References

- Abdi H., Williams, L.J. 2010. Principal Component Analysis. Wiley Interdisciplinary Reviews: Computational Statistics 2, 433-459.
- Abedi M., Mostafavi Kashani, S. B., Norouzi, G. H., Yousefi, M. 2017. A deposit scale mineral prospectivity analysis: A comparison of various knowledge-driven approaches for porphyry copper targeting in Seridune, Iran. *Journal of African Earth Sciences* 128, 127-146.
- Afzal, P., Khakzad, A., Moarefvand, P., Rashidnejad Omran, N., Esfandiari, B., Fadakar Alghalandis, Y. 2010. Geochemical anomaly separation by multifractal modeling in Kahang (Gor Gor) porphyry system, Central Iran. *Journal of Geochemical Exploration* 104, 34-46.
- Afzal, P., Zarifi, A.Z., Khankandi, S.F., Wetherelt, A., Yasrebi, A.B. 2012. Separation of uranium anomalies based on geophysical airborne analysis by using Concentration-Area (C-A) Fractal Model, Mahneshan 1:50000 Sheet, NW IRAN. *Journal of Mining and Metallurgy* 48A(1), 1-11.
- Aghazadeh, M. 2014. Geological report of Sonajeel (1:5000), Koome Madan Company.
- Aghazadeh, M., Hou, Z., Badrzadeh, Z., Zhou, L. 2015. Temporal-spatial distribution and tectonic setting of porphyry copper deposits in Iran: Constraints from zircon U-Pb and molybdenite Re-Os geochronology. *Ore Geology Reviews* 70, 385-406.
- Agterberg, F.P., Bonham-Carter, G.F., Wright, D.F. 1990. Statistical pattern integration for mineral exploration. In: Gaal G., Merriam D.F. (Eds.), *Computer Applications in Resource Estimation Prediction and Assessment for Metals and Petroleum*. Pergamon Press, Oxford New York, 1-21.
- Alimohammadi, M., Alirezaei, S., Kontak, D.J. 2015. Application of ASTER data for exploration of porphyry copper deposits: A case study of Daraloo-Sarmeshk area, southern part of the Kerman copper belt, Iran, *Ore Geology Reviews* 70, 290-304.
- Almasi, A., Jafarirad, A., Afzal, P., Rahimi, M. 2015a. Prospecting of gold mineralization in Saez area (NW Iran) using geochemical, geophysical and geological studies based on multifractal modelling and principal component analysis. *Arabian Journal of Geosciences* 8(8), 5935-5947.
- Almasi, A., Jafarirad, A., Kheirollahi, H., Rahimi, M., Afzal, P. 2015b. Orogenic Gold Prospectivity Mapping of Region Saez, *Bulletin of the Mineral Research and Exploration* 150, 65-76.
- Almasi, A., Yousefi, M., Carranza, E.J.M. 2017. Prospectivity analysis of orogenic gold deposits in Saez-Sardasht Goldfield, Zagros Orogen, Iran. *Ore Geology Reviews* 91, 1066-1080.
- An, P., Moon, W.M., Rencz, A. 1991. Application of fuzzy set theory to integrated mineral exploration. *Canadian Journal of Exploration Geophysics*, 27(1), 1-11.
- Babaie, H.A., Ghazi, A.M., Babaei, A., La Tour, T.E., Hassanipak, A.A. 2001. Geochemistry of arc volcanic rocks of the Zagros crush zone, Neyriz, Iran. *Journal of Asian Earth Sciences* 19, 61-76.
- Beane, R. E. 1982. Hydrothermal alteration in silicate rocks, in Tittley S. R., ed., *Advances in geology of the porphyry copper deposits, southwestern North America: Tucson*. The University of Arizona Press, pp. 117-137.
- Berberian, M., King, G.C. 1981. Towards a paleogeography and tectonic evolution of Iran. *Canadian Journal of Earth Sciences* 18, 210-265.
- Berger, B.R., Ayuso, R. A., Wynn, J.C., Seal, R.R. 2008. Preliminary Model of Porphyry Copper Deposits. USGS, Open-File Report, 1321 pp.
- Bishop, C.M. 2006. *Pattern Recognition and Machine Learning*. Springer: New York, NY, USA, 738 pp.
- Bonham-Carter, G.F. 1994. *Geographic Information Systems for Geoscientists: Modeling with GIS*. Pergamon Press, Ontario, Canada, 398 pp.
- Bonham-Carter, G.F., Agterberg, F.P., Wright, D.F. 1989. Weights of evidence modelling: new approach to mapping mineral potential In: Agterberg F. P., Bonham-Carter G. F. (Eds.), *Statistical Applications in the Earth Sciences Geological Survey of Canada*, 171-183.
- Byron, R., Berger Robert, A. 2008. Preliminary model of porphyry copper deposits, U.S. Geological survey 3.
- Carranza, E.J.M. 2008. Geochemical anomaly and mineral prospectivity mapping in GIS. *Handbook of Exploration and Environmental Geochemistry*, Vol. 11. Elsevier, Amsterdam.
- Carranza, E.J.M. 2009a. Mapping of anomalies in continuous and discrete fields of stream sediment geochemical landscapes. *Geochemistry: Exploration, Environment, Analysis* 10, 171-187.
- Carranza, E.J.M. 2009b. Controls on mineral deposit occurrence inferred from analysis of their spatial pattern and spatial association with geological features. *Ore Geology Reviews* 35, 383-400.
- Carranza, E.J.M. 2010. Improved Wildcat Modelling of Mineral Prospectivity. *Resource Geology* 60(2), 129-149.

- Carranza, E.J.M. 2014. Data-driven evidential belief modeling of mineral potential using few prospects and evidence with missing values. *Natural Resources* 24(3), 291-304.
- Carranza, E.J.M., Hall, M. 2002. Mineral mapping with Landsat thematic mapper data for hydrothermal alteration mapping in heavily vegetated terrane. *International Journal of Remote Sensing* 23(22), 4827-4852.
- Cheng, Q., Agterberg, F.P., Ballantyne, S.B. 1994. The separation of geochemical anomalies from background by fractal methods. *Journal of Geochemical Exploration* 51(2), 109-130.
- Chung, C.F., Agterberg, F.P. 1980. Regression models for estimating mineral resources from geological map data. *Mathematical Geology* 12(5), 472-488.
- Chung, C.F., Moon, W.M. 1990. Combination rules of spatial geoscience data for mineral exploration. *Geoinformatics* 2, 159-169.
- Davis, J.C. 2002. *Statistics and Data Analysis in Geology*, 3rd edn. John Wiley & Sons Inc, New York, pp. 342-353.
- Deng, J., Wang Q.F., Wan L., Yang L.Q., Liu X.F. 2007. Singularity of Au distribution in alteration rock type deposit, an example from Dayingezhuang gold ore deposit. In: Zhao P.D., Agterberg F., Cheng Q.M. (Eds.), *The 12th Conference of the International Association for Mathematical Geology*, China University of Geosciences Press, Wuhan, pp. 44-47.
- Deng, J., Wang, Q. F., Wan, L., Yang, L.Q., Zhou, L., Zhao, J. 2008. The random difference of the trace element distribution in skarn and marbles from Shizishan ore field, Anhui Province, China. *Journal of China University of Geosciences* 19(4), 123-137.
- Ford, A., Miller, J.M., Mol, A.G. 2015. A comparative analysis of weights of evidence, evidential belief functions, and fuzzy logic for mineral potential mapping using incomplete data at the scale of investigation. *Natural Resources Research* 25(1), 19-33.
- Hassanpour, Sh., Afzal, P. 2013. Application of concentration-number (C-N) multifractal modelling for geochemical anomaly separation in Haftcheshmeh porphyry system, NW Iran. *Arabian Journal of Geosciences* 6(3), 957-970.
- Hezarkhani, A. 2008. Hydrothermal Evolution of the Sonajil Porphyry Copper System, East Azarbaijan Province, Iran: The History of an Uneconomic Deposit. *International Geology Review* 50(5), 483-501.
- Hosseinzadeh, G. H., Mouayed, M., Esfahanipour, R. 2009. Supergene Processes in Sonajil Porphyry Copper Deposit With Respect To Using Of Leached Capping For Estimation of Supergene Enrichment in Porphyry Copper Deposits. *Iranian Journal Of Geology Summer*, Volume 3, Number 10; Page(s) 85 To 96.
- Hosseinzadeh, M.R., Maghfouri, S., Ghorbani, M., Moayyed, M. 2017. Different types of vein-veinlets related to mineralization and fluid inclusion studies in the Sonajil porphyry Cu- Mo deposit, Arasbaran magmatic zone. *Scientific Quarterly Journal geosciences* 26(101), 219-230.
- Jafarirad, A. 2009. Modeling of conceptual and empirical geospatial datasets for mineral prospecting mapping. PhD thesis, TUC, Germany, 190 pp.
- Jafarirad, A., Busch, W. 2011. Porphyry copper prospectivity mapping using interval valued fuzzy sets TOPSIS method in Central Iran. *International Journal of Geographical Information Science* 3, 312-317.
- Jamali, H., Mehrabi, B. 2015. Relationships between arc maturity and Cu-Mo-Au porphyry and related epithermal mineralization at the Cenozoic Arasbaran Magmatic Belt. *Ore Geology Reviews* 65(2), 487-501.
- Joly A., Porwal, A., McCuaig, T. C. 2012. Exploration targeting for orogenic gold deposits in the Granites-Tanami Orogen: Mineral system analysis, targeting model and prospectivity analysis. *Ore Geology Reviews* 48, 349-383.
- Karimi, M., Valadan Zoj, M.J. 2009. Mineral Potential Modeling of Sonajil Copper Prospect Using Fuzzy logic and GIS. *Materials and Energy. Quarterly Journal of Science Kharazmi University* 8(3), 265-282.
- Karimzadeh Somarin, A. 2005. Petrology and geochemistry of early tertiary volcanism of the Mendejin area, Iran, and implications for magma genesis and tectonomagmatic setting. *Geodinamica Acta* 18(5), 343-362.
- Lisitsin, V.A., González-Álvarez, I., Porwal, A. 2013. Regional prospectivity analysis for hydrothermal-remobilized nickel mineral systems in western Victoria, Australia. *Ore Geology Reviews* 52, 100-112.
- Lowell, J.D., Guilbert, J.M. 1970. Lateral and vertical alteration-mineralization zoning in porphyry ore deposits. *Economic Geology* 65(4), 373-408.
- Lusty, P.A.J., Scheib, C., Gunn, A.G., Walker, A. S. D. 2012. Reconnaissance-scale prospectivity analysis for gold mineralization in the Southern Uplands-Down-Longford Terrane, Northern Ireland. *Natural Resources Research* 21(3), 359-382.

- Magalhaes, L.A., Souza Filho, C.R. 2012. Targeting of gold deposits in Amazonian exploration frontiers using knowledge- and data-driven spatial modeling of geophysical, geochemical and geological data. *Surveys in Geophysics* 33(2), 211-214.
- McInnes, B.I.A., Evans, N.J., Belousova, E., Griffin, W. T., Andrew R. L. 2003. Timing of mineralization and exhumation processes at the Sar Cheshmeh and Meiduk porphyry Cu deposits, Kerman belt, Iran. In: Eliopoulos, et al. (Eds.), *Mineral Exploration and Sustainable Development (7th Biennial SGA Meeting, Athens (August 24–28))*. Millpress, Rotterdam, pp. 1197-1200
- Meyer, C., Hemley, J.J. 1967. Wall rock alteration, in Barnes H. L. ed., *Geochemistry of hydrothermal ore deposits*: New York, Holt, Rinehart and Winston, p. 166-235.
- Moritz, R., Rezeau, H., Ovtcharova, M., Tayan, R., Melkonyan, R., Hovakimyan, S., Ramazanov, V., Selby, D., Ulianov, A., Chiaradia, M., Pulitz, B. 2015. Long-lived, stationary magmatism and pulsed porphyry systems during Tethyan subduction to post-collision evolution in the southernmost Lesser Caucasus, Armenia and Nakhitchevan. *Durham Research Online*, <http://dx.doi.org/10.1016/j.gr.2015.10.009>.
- Nykanen, V., Groves, D.L., Ojala, V.J., Eilo, P., Gardoll, S.J. 2008. Reconnaissance scale conceptual fuzzy-logic prospectivity modelling for iron oxide copper-gold deposits in the northern Fennoscandian Shield, Finland. *Australian Journal of Earth Sciences* 55(1), 25-38.
- Parsa, M., Maghsoudi, A., Yousefi, M., Sadeghi, M. 2016. Prospectivity modeling of porphyry-Cu deposits by identification and integration of efficient mono-elemental geochemical signatures. *Journal of African Earth Sciences* 114, 228-241.
- Parsa, M., Maghsoudi, A., Yousefi, M. 2017. An improved data-driven fuzzy mineral prospectivity mapping procedure; cosine amplitude-based similarity approach to delineate exploration targets. *International Journal of Applied Earth Observation and Geoinformation* 58, 157-167.
- Pazand, K., Hezarkhani, A., Ataei, M. 2012. Using TOPSIS approaches for predictive porphyry Cu potential mapping: A case study in Ahar-Arasbaran area (NW, Iran), *Computers and Geosciences* 49 (2012) 62–71.
- Pazand, K., Hezarkhani, A., Ataei, M. 2013. The application of litho-geochemical and alteration index for copper mineralization in the Sonajil area, NW Iran. *Arabian Journal of Geosciences* 6(5), 1447-1456.
- Porwal, A., Kreuzer, O.P. 2010. Introduction to the Special Issue: Mineral prospectivity analysis and quantitative resource estimation. *Ore Geology Reviews* 38(3), 121-127.
- Porwal, A., Carranza, E.J.M. 2015. Introduction to the Special Issue: GIS-based mineral potential modelling and geological data analyses for mineral exploration. *Ore Geology Reviews* 71, 477-483.
- Richards, J.P. 2015. Tectonic, magmatic, and metallogenic evolution of the Tethyan orogen: From subduction to collision. *Ore Geology Reviews* 70, 323-345.
- Richards, J.P., Sholeh, A. 2016. Chapter 7- The Tethyan Tectonic History and Cu-Au Metallogeny of Iran. *Economic Geologists, Inc. Special Publication* 19, 193-212.
- Seedorff, E., Dilles, J.H., Phoffett, Jr., J.M., Einaudi, M.T., Zurcher, L., Stavast, W.J.A., Johnson, D.A., Barton, M.D. 2005. *Porphyry deposits: Characteristics and origin of hypogene features*. Littleton. *Economic Geology One Hundredth Anniversary Volume*, 251-298.
- Sillitoe, R.H. 2010. Porphyry copper systems. *Economic Geology* 105, 3-41.
- Shahabpour, J., Kramers, J.D. 1987. Lead isotope data from the Sar Cheshmeh porphyry copper deposit, Kerman. Iran. *Mineralium Deposita* 22, 278-281.
- Stocklin, J. 1974. Possible ancient continental margins in Iran. In: Burk, C.A., Drake, C.L. (Eds.), *The Geology of Continental Margins*. Springer, Berlin, pp. 873-887.
- Tsoukalas, L.H., Uhrig, R.E. 1997. *Fuzzy and neural approaches in engineering*. Wiley, New York, p 587.
- Wang, Y.M., Chin, K.S. 2011. Fuzzy data envelopment analysis: A fuzzy expected value approach. *Expert Systems with Applications* 38(9), 11678-11685.
- Wang, G., Zhu, Y., Zhang, S., Yan, C., Song, Y., Ma, Z., Hong, D., Chen, T. 2012. 3D geological modeling based on gravitational and magnetic data inversion in the Luanchuan ore region, Henan Province, China. *Journal of Applied Geophysics* 80, 1-11.
- Wang, G., Pang, Z., Boisvert, J.B., Hao, Y., Cao, Y., Qu, J. 2013. Quantitative assessment of mineral resources by combining geostatistics and fractal methods in the Tongshan porphyry Cu deposit (China). *Journal of Geochemical Exploration* 134, 85-98.
- Wang, W., Zhao, J., Cheng, Q., Carranza, E.J.M. 2014. GIS-based mineral potential modeling by advanced spatial analytical methods in the southeastern Yunnan mineral district, China. *Ore Geology Reviews* 71, 735-748.

- Yazdi, Z., Jafarirad, A.R., Ajayebi, K.S. 2014. Analysis and modeling of geospatial datasets for porphyry copper prospectivity mapping in Chahargonbad area, Central Iran. *Arabian Journal of Geosciences* 8(10), 8237-8248.
- Yousefi, M. 2017. Recognition of an enhanced multi-element geochemical signature of porphyry copper deposits for vectoring into mineralized zones and delimiting exploration targets in Jiroft area, SE Iran. *Ore Geology Reviews* 83, 200-214.
- Yousefi, M., Kamkar-Rouhani, A., Carranza, E.J.M. 2012. Geochemical mineralization probability index (GMPI): a new approach to generate enhanced stream sediment geochemical evidential map for increasing probability of success in mineral potential mapping. *Journal of Geochemical Exploration* 115, 24-35.
- Yousefi, M., Carranza, E.J.M., Kamkar-Rouhani, A. 2013. Weighted drainage catchment basin mapping of stream sediment geochemical anomalies for mineral potential mapping. *Journal of Geochemical Exploration* 128, 88-96.
- Yousefi, M., Carranza, E.J.M. 2014. Data-driven index overlay and Boolean logic mineral prospectivity modeling in greenfields exploration. *Natural Resources Research* 25(1), 3-18.
- Yousefi, M., Carranza, E.J.M. 2015a. Fuzzification of continuous-value spatial evidence for mineral prospectivity mapping. *Computers and Geosciences* 74, 97-109.
- Yousefi, M., Carranza, E.J.M. 2015b. Prediction-area (P-A) plot and C-A fractal analysis to classify and evaluate evidential maps for mineral prospectivity modeling. *Computers and Geosciences* 79, 69-81.
- Yousefi, M., Nykanen, V. 2016. Data-driven logistic-based weighting of geochemical and geological evidence layers in mineral prospectivity mapping. *Journal of Geochemical Exploration* 164, 94-106.